Supporting Information for

"*In-vitro* Replication Studies on O^2-Methylthymidine and O^4-Methylthymidine"

Nisana Andersen[1], Jianshuang Wang[1], Pengcheng Wang[2], Yong Jiang[2] and Yinsheng Wang[1,2,*]

[1]Department of Chemistry and [2]Environmental Toxicology Graduate Program, University of California, Riverside, California 92521-0403

Chem. Res. Toxicol., 2012

Figure S1. Product-ion spectrum of the $[M-4H]^{4-}$ ion (*m/z* 1300.4) of the 17-mer ODN d(CCATGGCA*X*GAGAATTC), where "*X*" is O^2-MdT (A) and O^4-MdT (B). Shown in the inset is the negative-ion ESI-MS for the ODNs.

Figure S2. Calibration curves for the ratios of unextended primer d(AATTCTC) to d(AATTCTCATGC) (i.e., 11A) (A); d(AATTCTCA) (i.e., 8A) to 11A (B); d(AATTCTCG) (i.e., 8G) to 11A (C); d(AATTCTCTGC) (i.e., 10Del) to 11A (D); d(AATTCTCCTGC) (i.e., 11C) to 11A (E); d(AATTCTCTTGC) (i.e., 11T) to 11A (F); d(AATTCTCGTGC) (i.e., 11G) to 11A (G).

Figure S3. Representative gel images for steady-state kinetic assays measuring nucleotide incorporation opposite undamaged dT (A), O^2-MdT (B), and O^4-MdT (C) with Kf $^-$ (0.7-7 nM). Reactions were conducted in the presence of individual dNTPs with the highest concentrations indicated in the figures. The ratios of dNTP concentrations were 0.5-0.6 between neighboring lanes.

Figure S4. Representative gel images for steady-state kinetic assays measuring nucleotide incorporation opposite undamaged dT (A), O^2-MdT (B), and O^4-MdT (C) with human DNA polymerase κ (1-5 nM). Reactions were conducted in the presence of individual dNTPs with the highest concentrations indicated in the figures. The concentration ratios of dNTP between neighboring lanes were 0.5-0.6.

Figure S5. Representative gel images for steady-state kinetic assays measuring nucleotide incorporation opposite undamaged dT (A), O^2-MdT (B), and O^4-MdT (C) with yeast polymerase η (7.5 nM). Reactions were conducted in the presence of individual dNTPs with the highest concentrations indicated in the figures. The concentration ratios of dNTP between neighboring lanes were 0.5-0.6.

Figure S6. (A) The total-ion chromatogram derived from the LC-MS/MS analysis of the human pol κ-induced replication products of O^2-MdT-containing substrates that have been treated with two restriction enzymes, NcoI and EcoRI plus shrimp alkaline phosphatase. (B) ESI-MS averaged from the peaks eluting in 18.5-20.5 min in part (A), where 'T*' designates the remnant of the digested template containing the damaged site, i.e., d(CATGGCA*X*GAG), where '*X*' is O^2-MdT, and 'P*' designates the 5' portion of the digested primer, i.e., d(GCTAGGATCATAG)

Figure S7. Analysis of the unextended primer and +1 extension products from the human pol κ-induced replication reaction arising from replication of O^2-MdT-containing substrates that have been treated with two restriction enzymes, NcoI and EcoRI, and shrimp alkaline phosphatase. Product-ion spectra of the ESI-produced $[M-2H]^{2-}$ ion of: the 7mer, d(AATTCTC) (precursor ion *m/z* 1026.2) (A); 8A, d(AATTCTCA) (precursor ion *m/z* 1182.7) (B); 8G, d(AATTCTCG) (precursor ion *m/z* 1190.7) (C); 10Del, d(AATTCTCTGC) (precursor ion *m/z* 1487.3) (D). In this and the following MS/MS figures, the arrow indicates the fragmentation process, and the solid and open circles represent the precursor ion and fragment ions, respectively.

Figure S8. Analysis of full-length extension products from the human pol κ-induced replication reaction arising from replication of O^2-MdT-containing substrates that have been treated with

two restriction enzymes, NcoI and EcoRI, and shrimp alkaline phosphatase. Product-ion spectra of the ESI-produced $[M-2H]^{2-}$ ions of: 11C, d(AATTCTCCTGC) (precursor ion *m/z* 1631.8) (A); 11T, d(AATTCTCTTGC) (precursor ion *m/z* 1639.3) (B); 11A, d(AATTCTCATGC) (precursor ion *m/z* 1643.8) (C); 11G, d(AATTCTCGTGC) (precursor ion *m/z* 1651.7) (D).

Figure S9. The selected-ion chromatograms (SICs) derived from the LC-MS/MS analysis of the replication mixture of the substrate containing dT with: Klenow fragment exo$^-$ (A), yeast pol η (B), and human pol κ (C).

Figure S10. The SICs derived from the LC-MS/MS analysis of the replication mixture of the substrate containing O^2-MdT with: Klenow fragment exo$^-$ (A), and yeast pol η (B).

Figure S11. The SICs derived from the LC-MS/MS analysis of the replication mixture of the substrate containing O^4-MdT with: Klenow fragment exo$^-$ (A), yeast pol η (B), and human pol κ (C).

Figure S12. LC-MS/MS for monitoring possible demethylation of O^2-MdT-containing template following primer extension with human pol κ and restriction digestion. Shown are the SICs derived from ultra-zoom scans monitoring the $[M-3H]^{3-}$ ions from the unmethylated and O^2-MdT 12mer arising from the digestion of the original O^2-MdT-containing template.

Figure S13. LC-MS/MS for monitoring possible demethylation of O^2-MdT-containing templates following primer extension with human pol κ. Shown are the product-ion spectra of the ESI-produced $[M-3H]^{3-}$ ions of: unmethylated 12mer, d(CATGGCCA**T**GAG) (precursor ion *m/z* 1221.9) (A); original 12mer, d(CATGGCCA[***O*^{2}-MdT**]GAG) (precursor ion *m/z* 1226.5) (B).

Figure S14. The SICs derived from the LC-MS/MS analysis of the replication mixture of the substrate containing O^4-MdT with yeast pol η: low dNTPs (A), 6 hr (B).

Figure S15. Representative gel images for steady-state kinetic assays measuring extension past undamaged dT (A), O^2-MdT (B), and O^4-MdT (C) with the base opposite the lesion indicated in the figure. Reactions were conducted with human polymerase κ (1-5 nM) in the presence of individual dNTPs with the highest concentrations indicated in the figures. The concentration ratios of dNTP between neighboring lanes were 0.5-0.6.

Table S1. Summary of the percentages of replication products produced for O^4-MdT-containing substrates by yeast pol η as determined by LC-ESI-MS/MS experiments. Reactions were conducted under two separate conditions: (1) low dNTPs concentrations (50 μM each) at 37°C overnight; (2) 1 mM dNTPs at 37°C for 6 hr. The template was d(CCATGGCA***X***GAGAATTCTATGATCCTAG), where ***'X'*** represents O^4-MdT.

Table S2. Efficiency and fidelity of human polymerase κ-mediated nucleotide extension with dATP and dGTP opposite undamaged dT, O^2-MdT and O^4-MdT as determined by steady-state kinetic measurements.

(A)

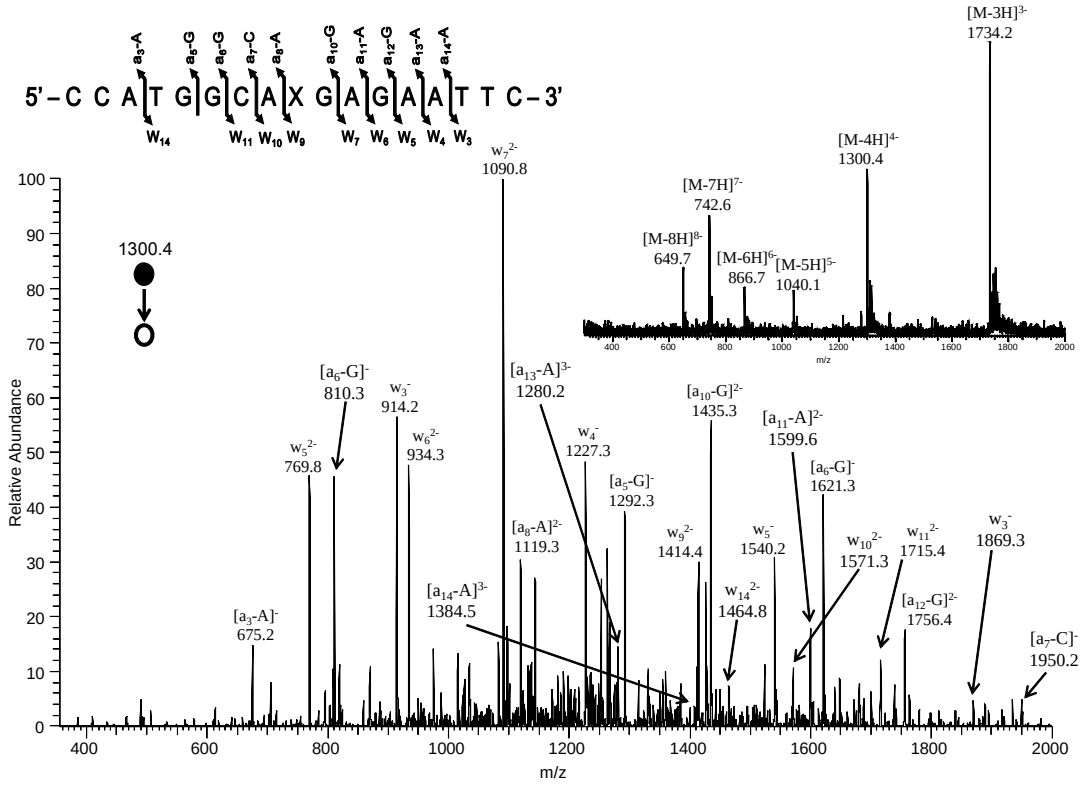
5'-C C A T G G C A X G A G A A T T C-3'
Relative Abundance
m/z
1300.4
[M-3H]3- 1734.2
[M-4H]4- 1300.4
[M-7H]7- 742.6
[M-8H]8- 649.7
[M-6H]6- 866.7
[M-5H]5- 1040.1
w7 2- 1090.8
[a6-G]- 810.3
w3- 914.2
w5 2- 769.8
w6 2- 934.3
[a13-A]3- 1280.2
w4- 1227.3
[a5-G]- 1292.3
[a10-G]2- 1435.3
[a11-A]2- 1599.6
[a6-G]- 1621.3
[a8-A]2- 1119.3
w9 2- 1414.4
w5- 1540.2
w10 2- 1571.3
w11 2- 1715.4
w3- 1869.3
[a14-A]3- 1384.5
w14 2- 1464.8
[a12-G]2- 1756.4
[a3-A]- 675.2
[a7-C]- 1950.2

(B)

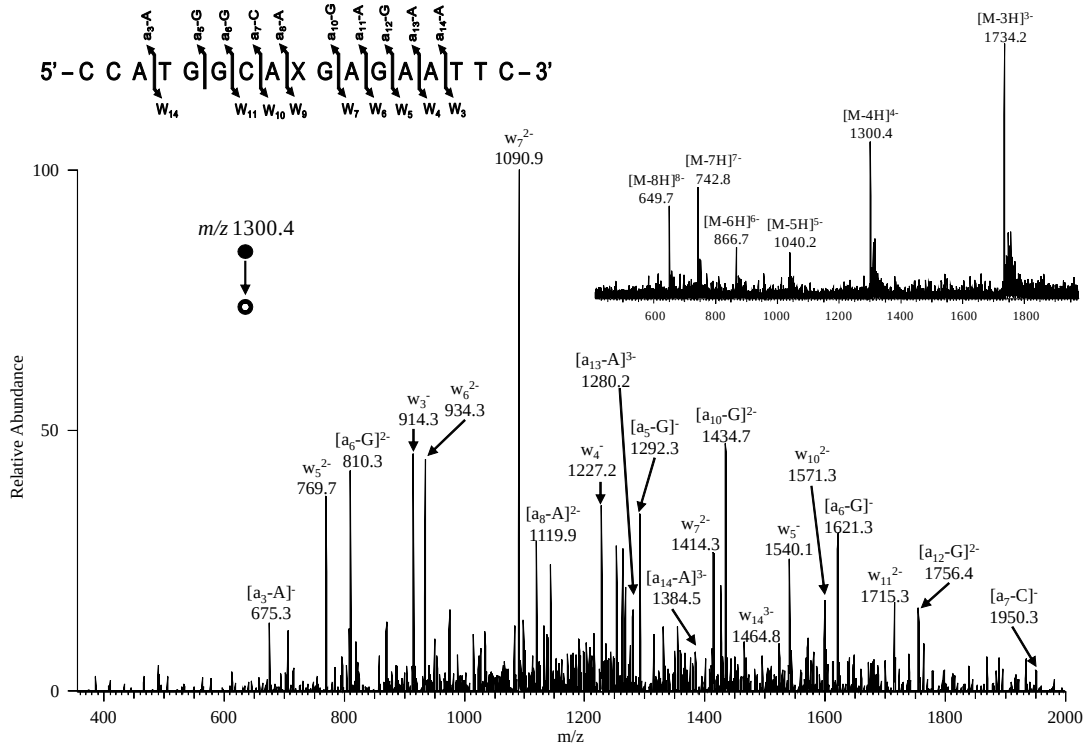
5'-C C A T G G C A X G A G A A T T C-3'
Relative Abundance
m/z
m/z 1300.4
[M-3H]3- 1734.2
[M-4H]4- 1300.4
[M-7H]7- 742.8
[M-8H]8- 649.7
[M-6H]6- 866.7
[M-5H]5- 1040.2
w7 2- 1090.9
[a13-A]3- 1280.2
[a5-G]- 1292.3
[a10-G]2- 1434.7
w3- 914.3
w6 2- 934.3
[a6-G]2- 810.3
w4- 1227.2
w5 2- 769.7
w10 2- 1571.3
[a6-G]- 1621.3
[a8-A]2- 1119.9
w7 2- 1414.3
w5- 1540.1
[a12-G]2- 1756.4
[a14-A]3- 1384.5
w11 2- 1715.3
w14 3- 1464.8
[a3-A]- 675.3
[a7-C]- 1950.3

Figure S1.

(A)

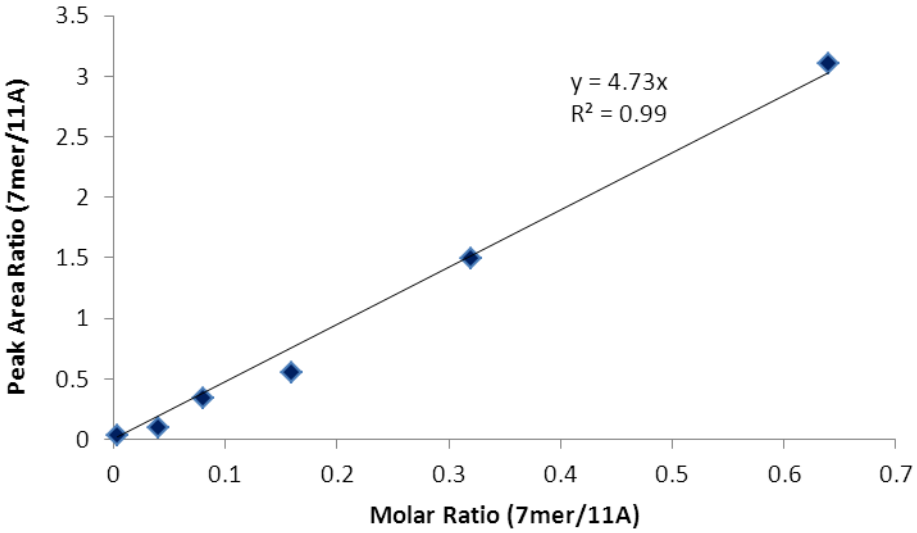
y = 4.73x
R² = 0.99
Peak Area Ratio (7mer/11A)
Molar Ratio (7mer/11A)
0
0.5
1
1.5
2
2.5
3
3.5
0
0.1
0.2
0.3
0.4
0.5
0.6
0.7

(B)

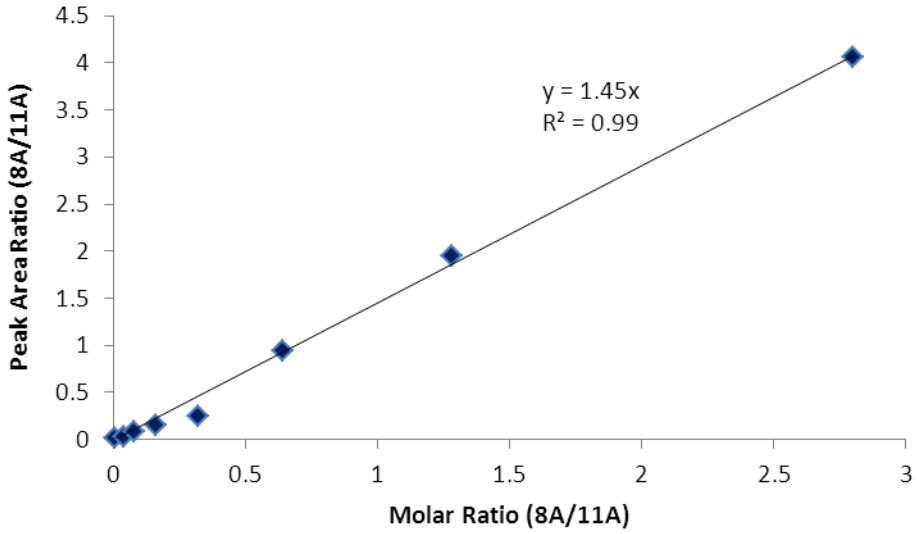
y = 1.45x
R² = 0.99
Peak Area Ratio (8A/11A)
Molar Ratio (8A/11A)
0
0.5
1
1.5
2
2.5
3
3.5
4
4.5
0
0.5
1
1.5
2
2.5
3

Figure S2.

(C)

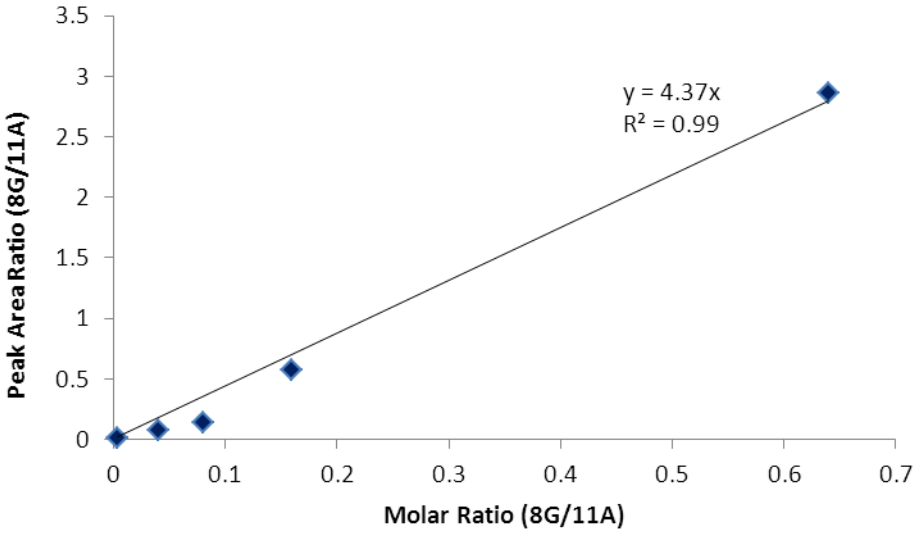
y = 4.37x
R² = 0.99
Peak Area Ratio (8G/11A)
Molar Ratio (8G/11A)
0
0.5
1
1.5
2
2.5
3
3.5
0
0.1
0.2
0.3
0.4
0.5
0.6
0.7

(D)

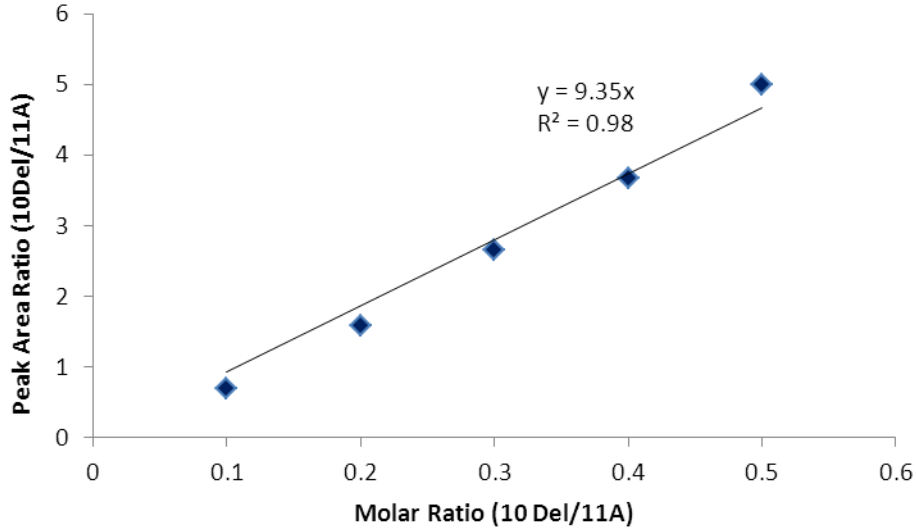
y = 9.35x
R² = 0.98
Peak Area Ratio (10Del/11A)
Molar Ratio (10 Del/11A)
0
1
2
3
4
5
6
0
0.1
0.2
0.3
0.4
0.5
0.6

Figure S2.

(E)

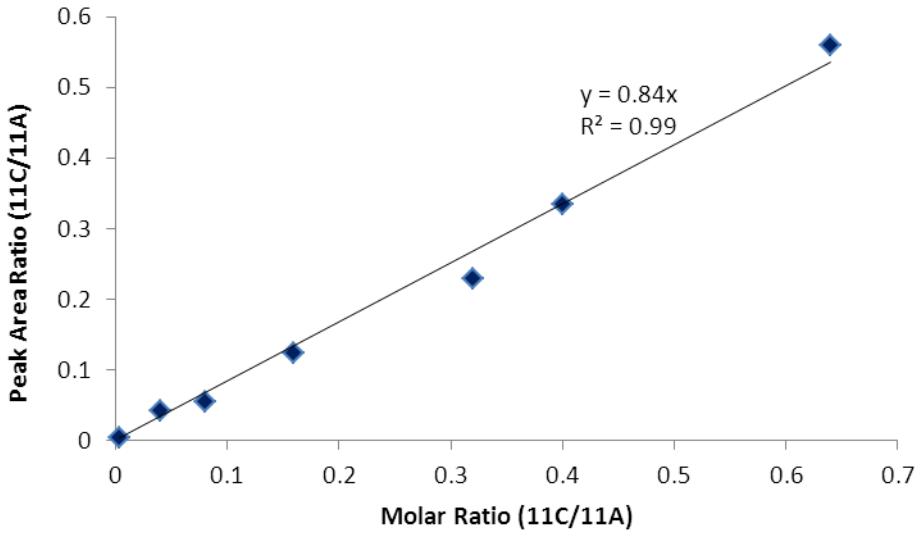
y = 0.84x
R² = 0.99
Peak Area Ratio (11C/11A)
Molar Ratio (11C/11A)
0
0.1
0.2
0.3
0.4
0.5
0.6
0.7

(F)

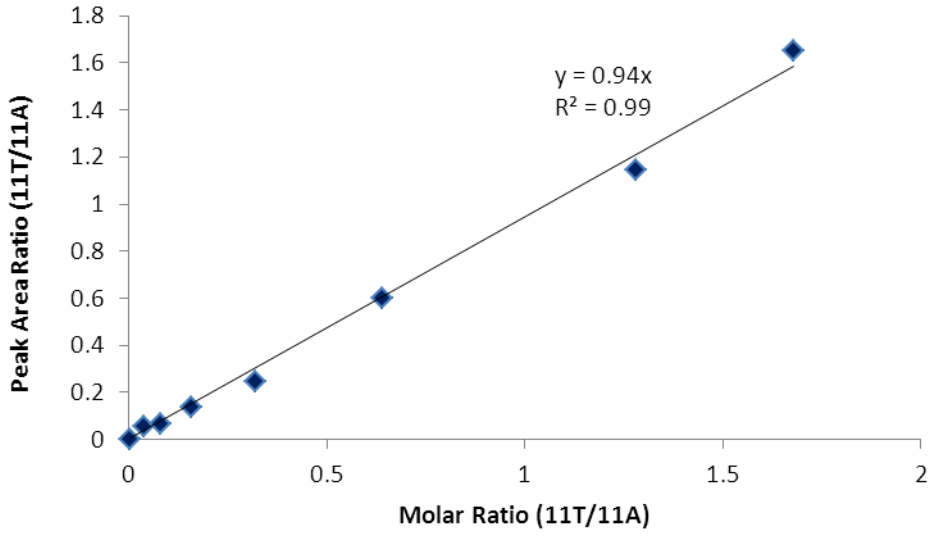
y = 0.94x
R² = 0.99
Peak Area Ratio (11T/11A)
Molar Ratio (11T/11A)
0
0.2
0.4
0.6
0.8
1
1.2
1.4
1.6
1.8
0.5
1.5
2

Figure S2.

(G)

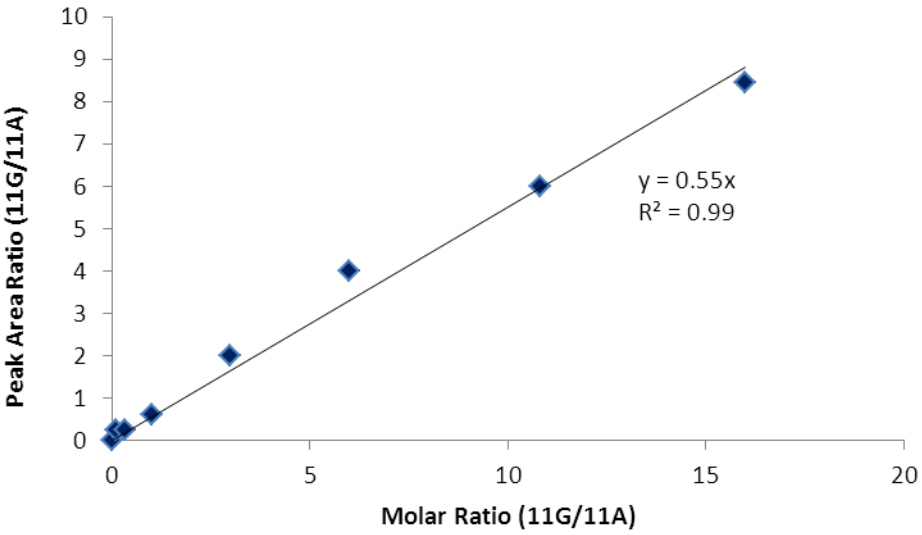
Peak Area Ratio (11G/11A)
Molar Ratio (11G/11A)
y = 0.55x
R² = 0.99
0
1
2
3
4
5
6
7
8
9
10
0
5
10
15
20

Figure S2.

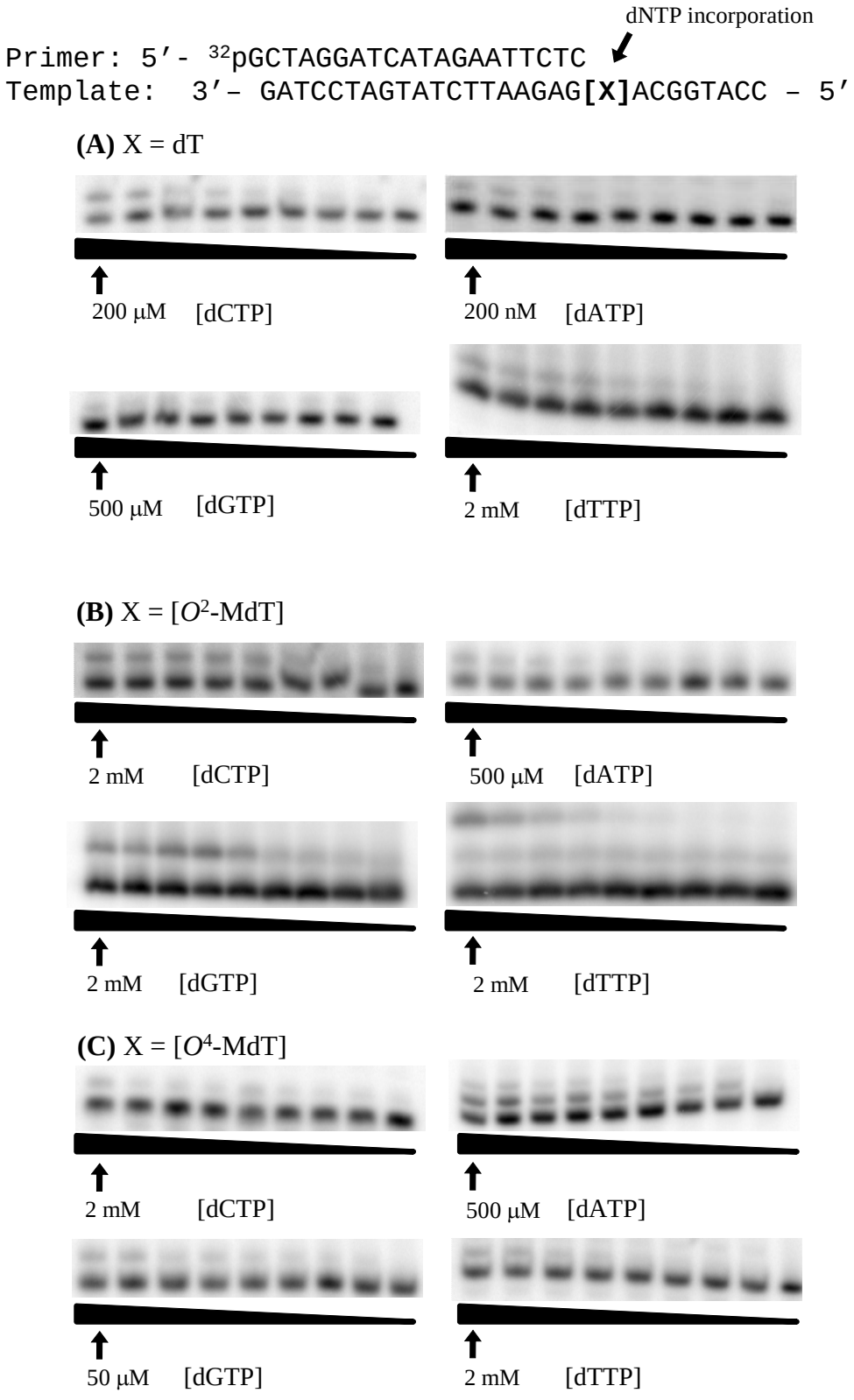
dNTP incorporation
Primer: 5′- 32pGCTAGGATCATAGAATTCTC
Template: 3′– GATCCTAGTATCTTAAGAG[X]ACGGTACC – 5′
(A) X = dT
200 μM [dCTP]
200 nM [dATP]
500 μM [dGTP]
2 mM [dTTP]
(B) X = [O2-MdT]
2 mM [dCTP]
500 μM [dATP]
2 mM [dGTP]
2 mM [dTTP]
(C) X = [O4-MdT]
2 mM [dCTP]
500 μM [dATP]
50 μM [dGTP]
2 mM [dTTP]

Figure S3.

Primer: 5′- ^{32}pGCTAGGATCATAGAATTCTC ↙
Template: 3′ – GATCCTAGTATCTTAAGAG**[X]**ACGGTACC – 5′

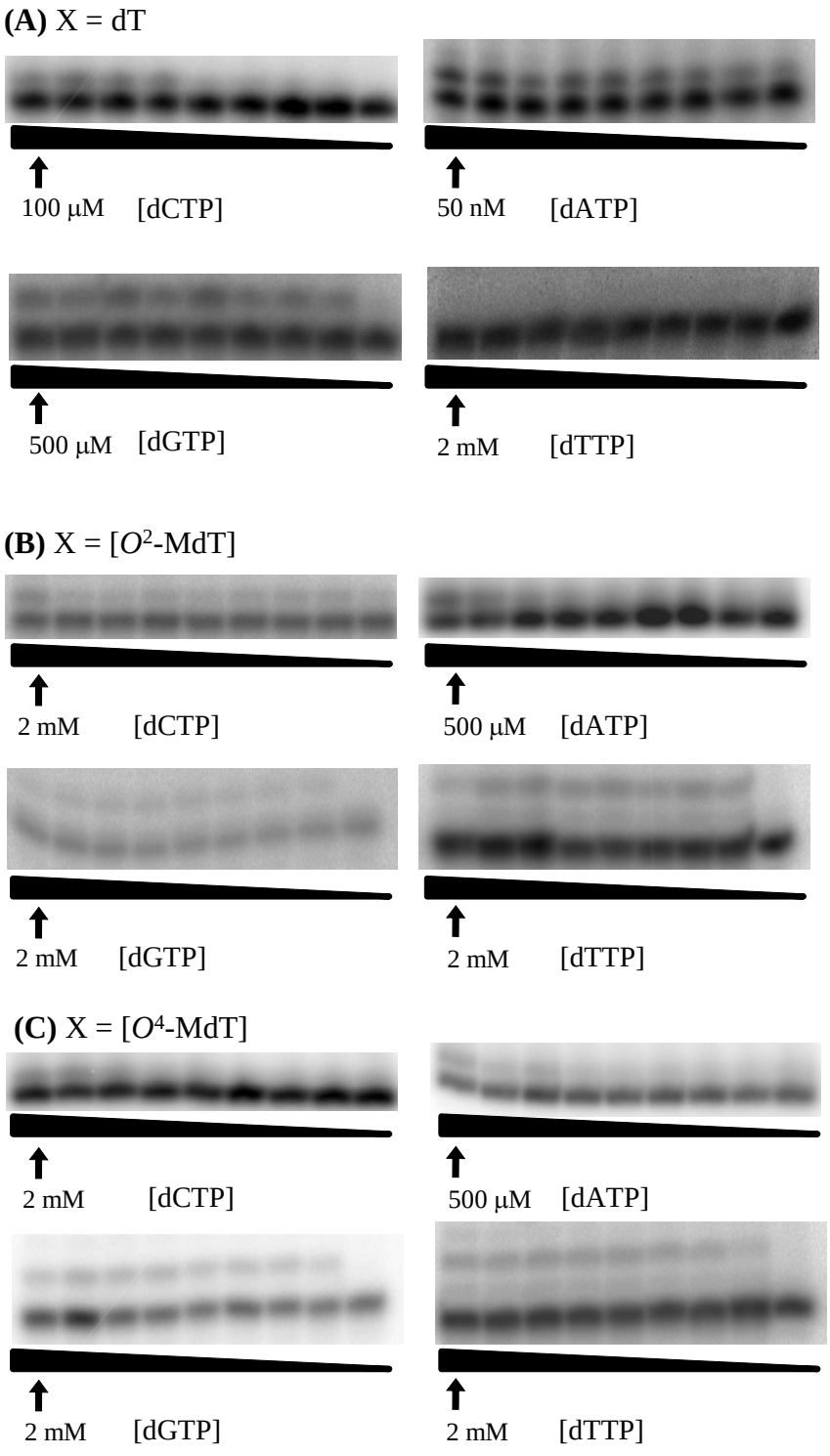

Figure S4.

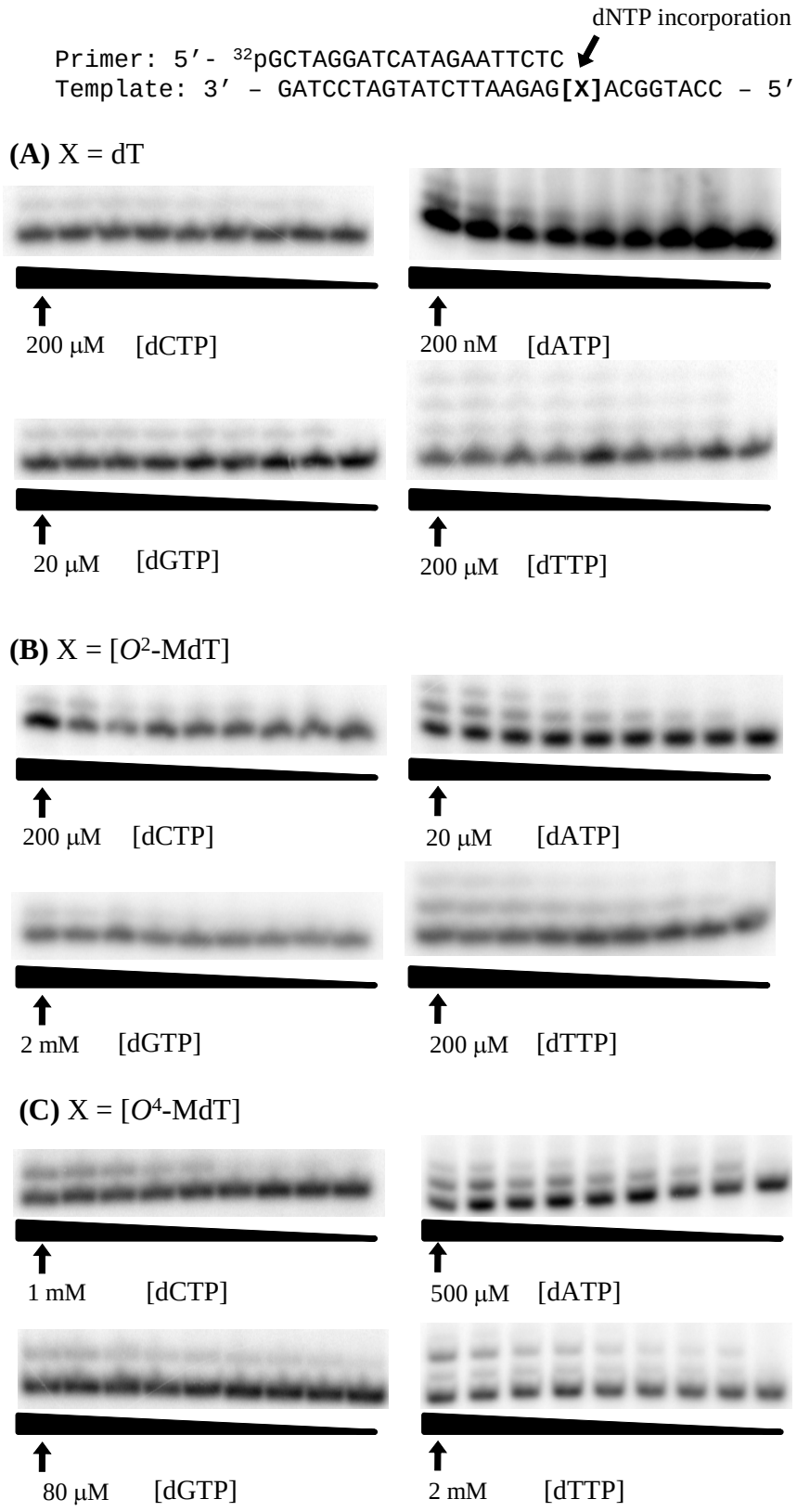
dNTP incorporation
Primer: 5′- 32pGCTAGGATCATAGAATTCTC
Template: 3′ – GATCCTAGTATCTTAAGAG[X]ACGGTACC – 5′
(A) X = dT
200 μM [dCTP]
200 nM [dATP]
20 μM [dGTP]
200 μM [dTTP]
(B) X = [O2-MdT]
200 μM [dCTP]
20 μM [dATP]
2 mM [dGTP]
200 μM [dTTP]
(C) X = [O4-MdT]
1 mM [dCTP]
500 μM [dATP]
80 μM [dGTP]
2 mM [dTTP]

Figure S5.

(A)

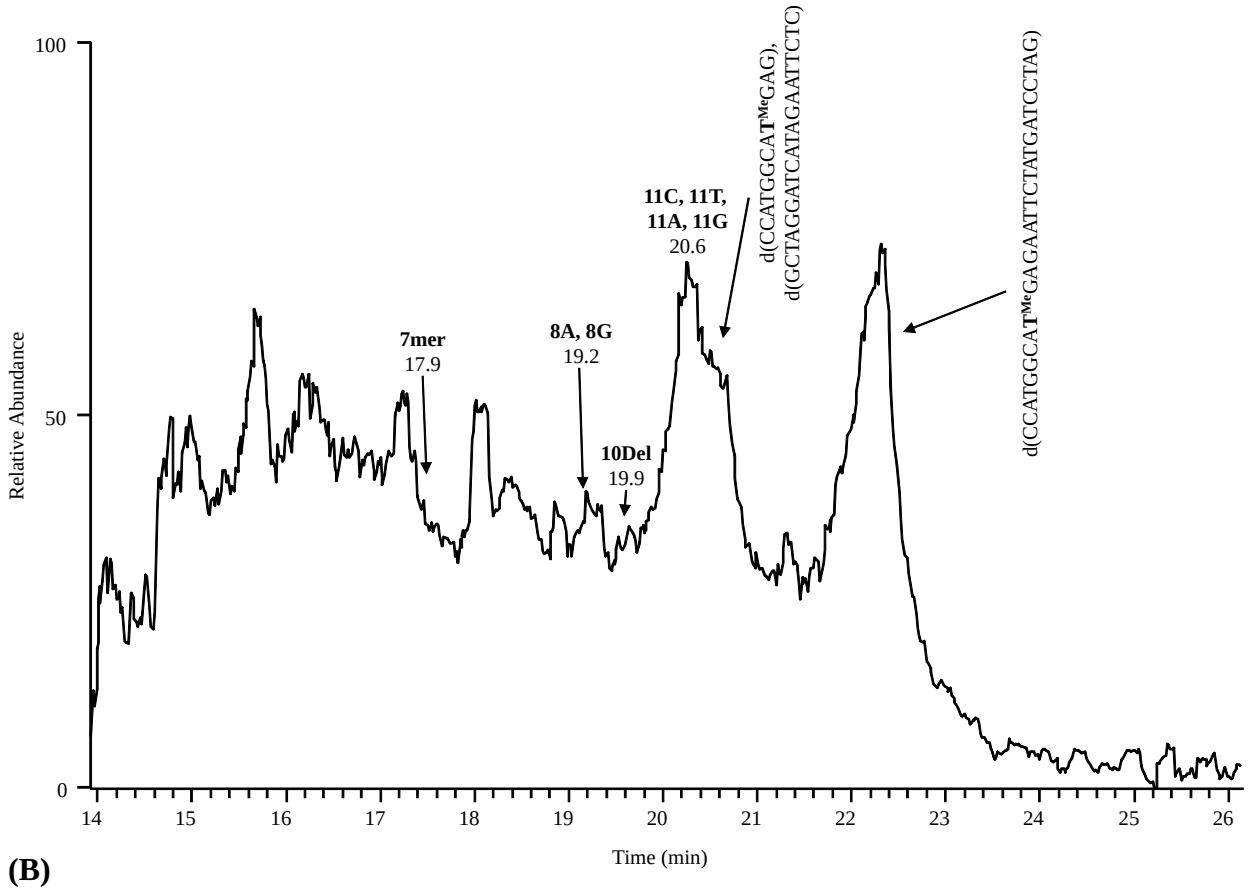
100
50
0
Relative Abundance
14
15
16
17
18
19
20
21
22
23
24
25
26
Time (min)
7mer
17.9
8A, 8G
19.2
10Del
19.9
11C, 11T,
11A, 11G
20.6
d(CCATGGCATMeGAG),
d(GCTAGGATCATAGAATTCTC)
d(CCATGGCATMeGAGAATTCTATGATCCTAG)

(B)

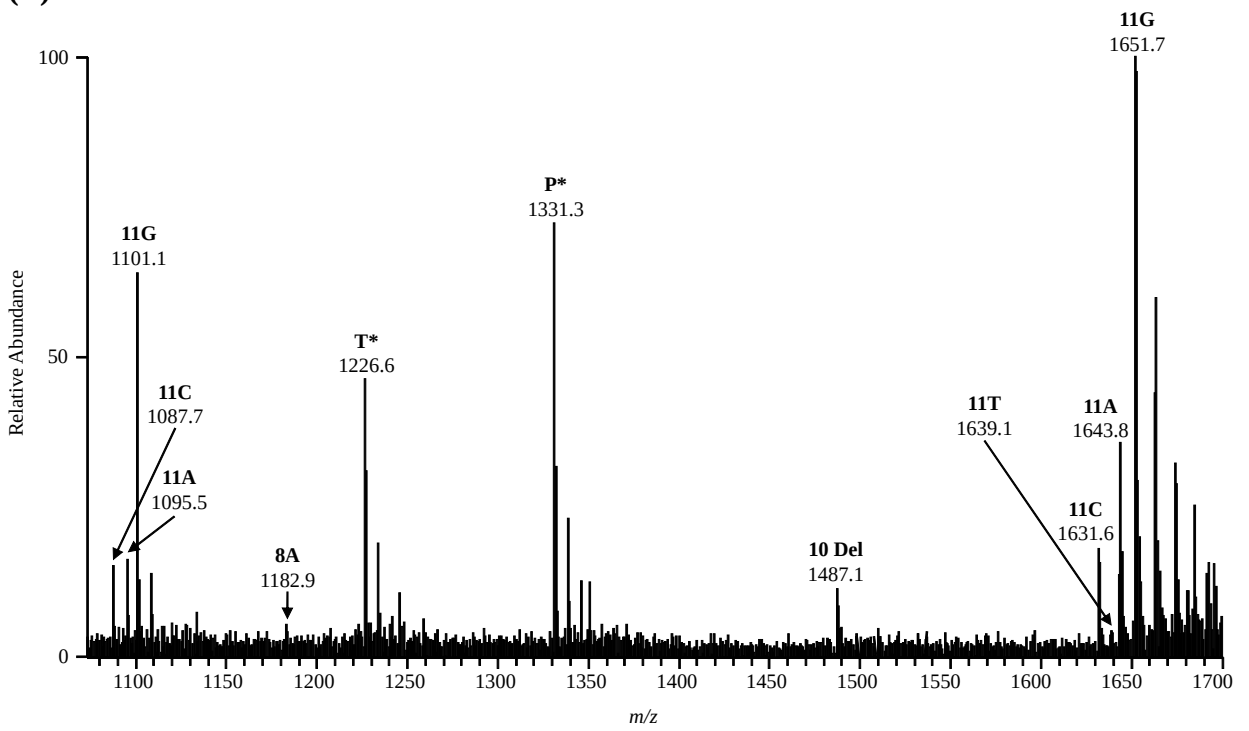
100
50
0
Relative Abundance
1100
1150
1200
1250
1300
1350
1400
1450
1500
1550
1600
1650
1700
m/z
11G
1101.1
11C
1087.7
11A
1095.5
8A
1182.9
T*
1226.6
P*
1331.3
10 Del
1487.1
11T
1639.1
11C
1631.6
11A
1643.8
11G
1651.7

Figure S6.

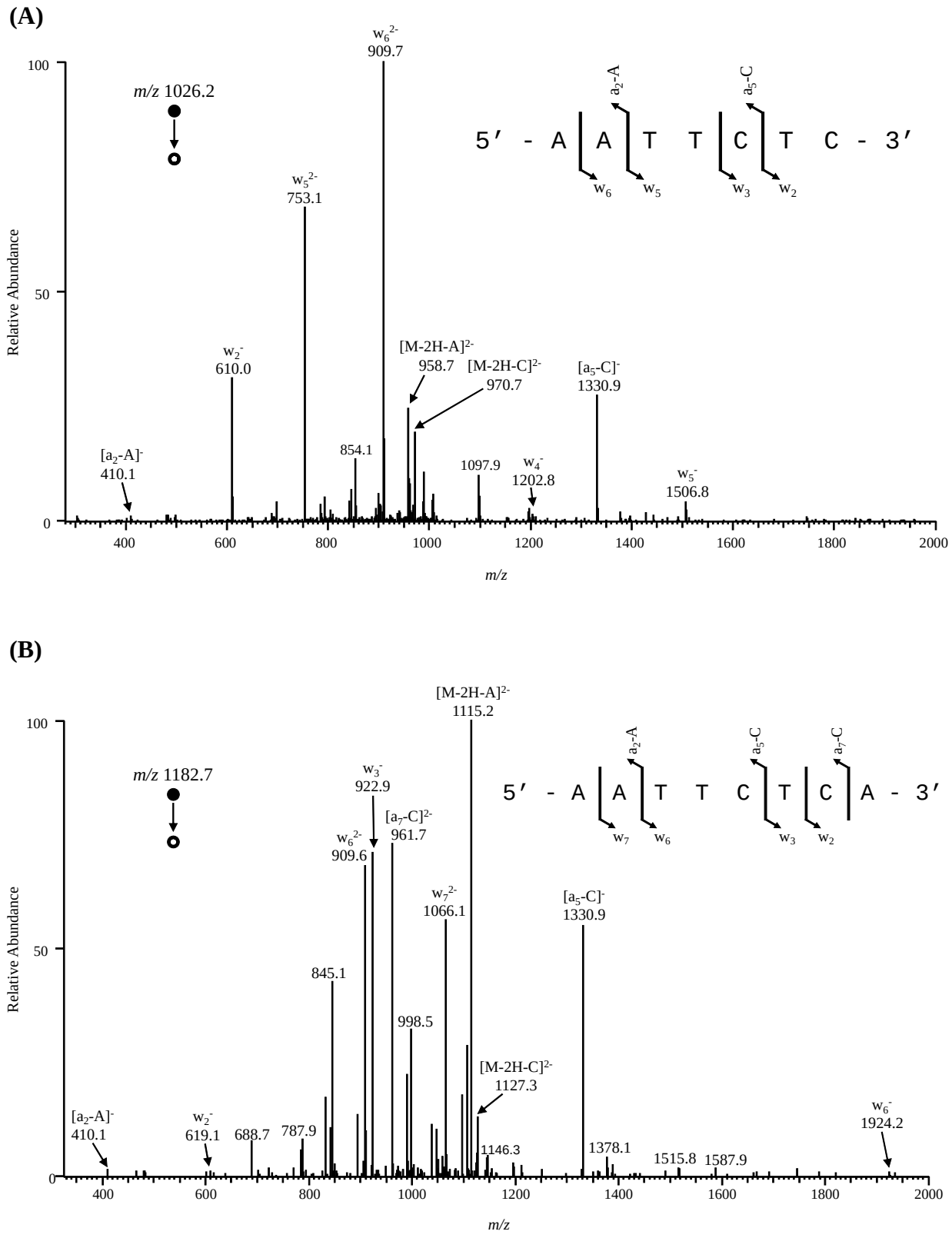
(A)
m/z 1026.2
5′ - A A T T C T C - 3′
a2-A
a5-C
w6
w5
w3
w2
w6 2- 909.7
w5 2- 753.1
w2- 610.0
[M-2H-A]2- 958.7
[M-2H-C]2- 970.7
[a5-C]- 1330.9
[a2-A]- 410.1
854.1
1097.9
w4- 1202.8
w5- 1506.8
Relative Abundance
m/z
(B)
m/z 1182.7
5′ - A A T T C T C A - 3′
a2-A
a5-C
a7-C
w7
w6
w3
w2
[M-2H-A]2- 1115.2
w3- 922.9
[a7-C]2- 961.7
w6 2- 909.6
w7 2- 1066.1
[a5-C]- 1330.9
845.1
998.5
[M-2H-C]2- 1127.3
[a2-A]- 410.1
w2- 619.1
688.7
787.9
1146.3
1378.1
1515.8
1587.9
w6- 1924.2
Relative Abundance
m/z

Figure S7.

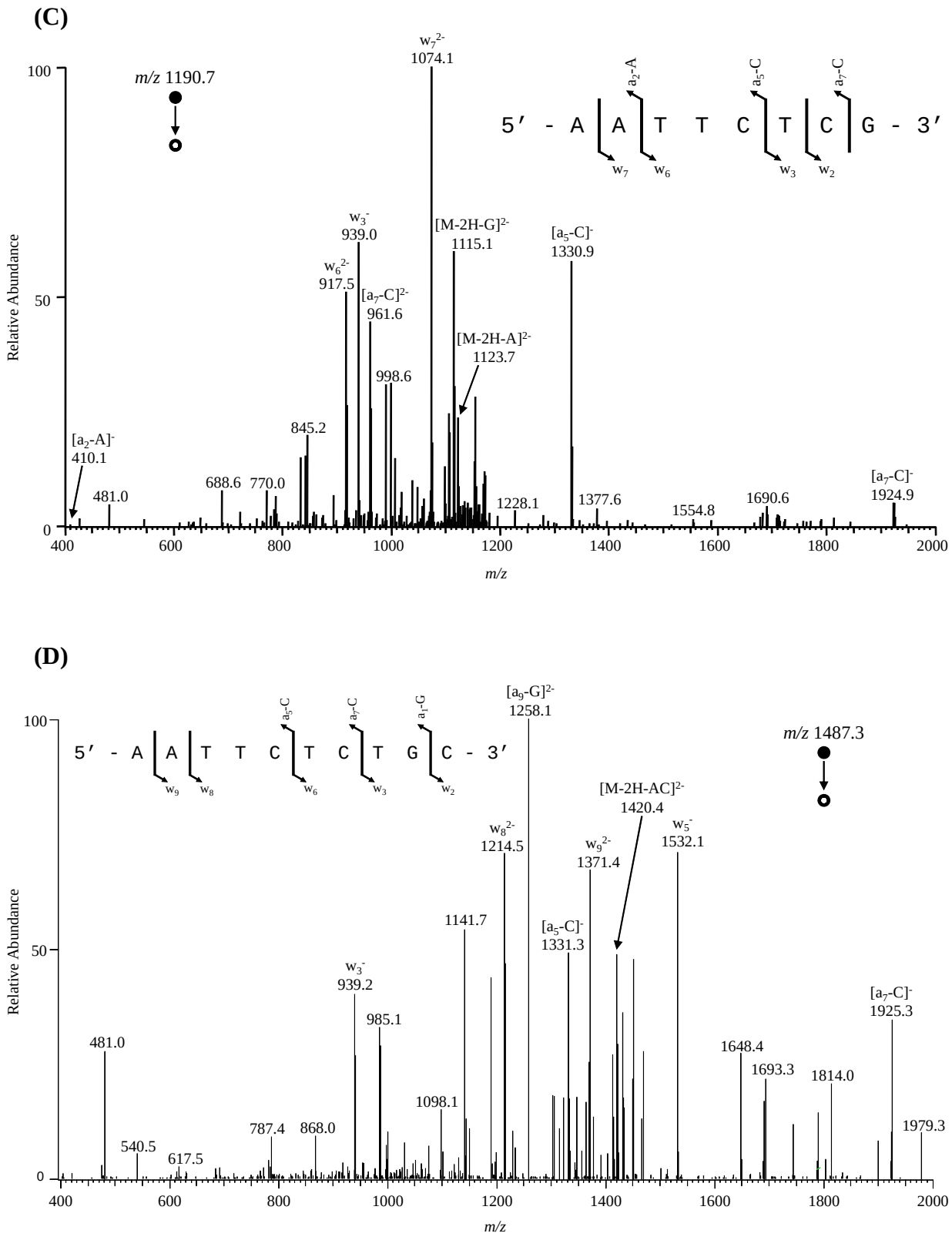
(C)
m/z 1190.7
5′ - A A T T C T C G - 3′
Relative Abundance
m/z
(D)
m/z 1487.3
5′ - A A T T C T C T G C - 3′
Relative Abundance
m/z

Figure S7.

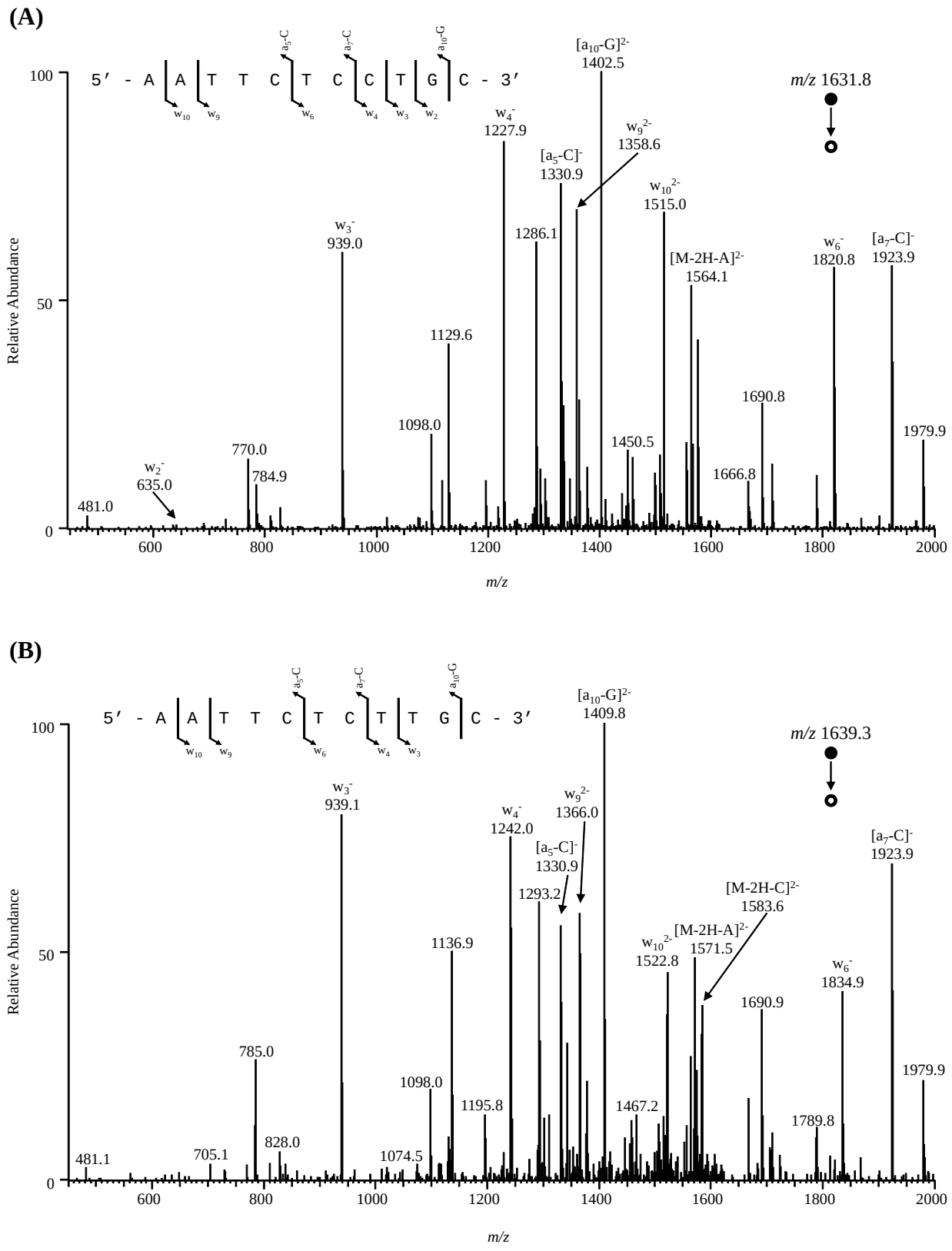
(A)
5′ - A A T T C T C C T G C - 3′
m/z 1631.8
[a10-G]2-
1402.5
w4-
1227.9
w92-
1358.6
[a5-C]-
1330.9
w102-
1515.0
w3-
939.0
1286.1
w6-
1820.8
[a7-C]-
1923.9
[M-2H-A]2-
1564.1
1129.6
1690.8
1098.0
1979.9
1450.5
770.0
w2-
635.0
784.9
1666.8
481.0
Relative Abundance
m/z
(B)
5′ - A A T T C T C T T G C - 3′
m/z 1639.3
[a10-G]2-
1409.8
w3-
939.1
w92-
1366.0
w4-
1242.0
[a5-C]-
1330.9
[a7-C]-
1923.9
1293.2
[M-2H-C]2-
1583.6
[M-2H-A]2-
1571.5
w102-
1522.8
1136.9
w6-
1834.9
1690.9
785.0
1979.9
1098.0
1195.8
1467.2
1789.8
828.0
481.1
705.1
1074.5
Relative Abundance
m/z

Figure S8.

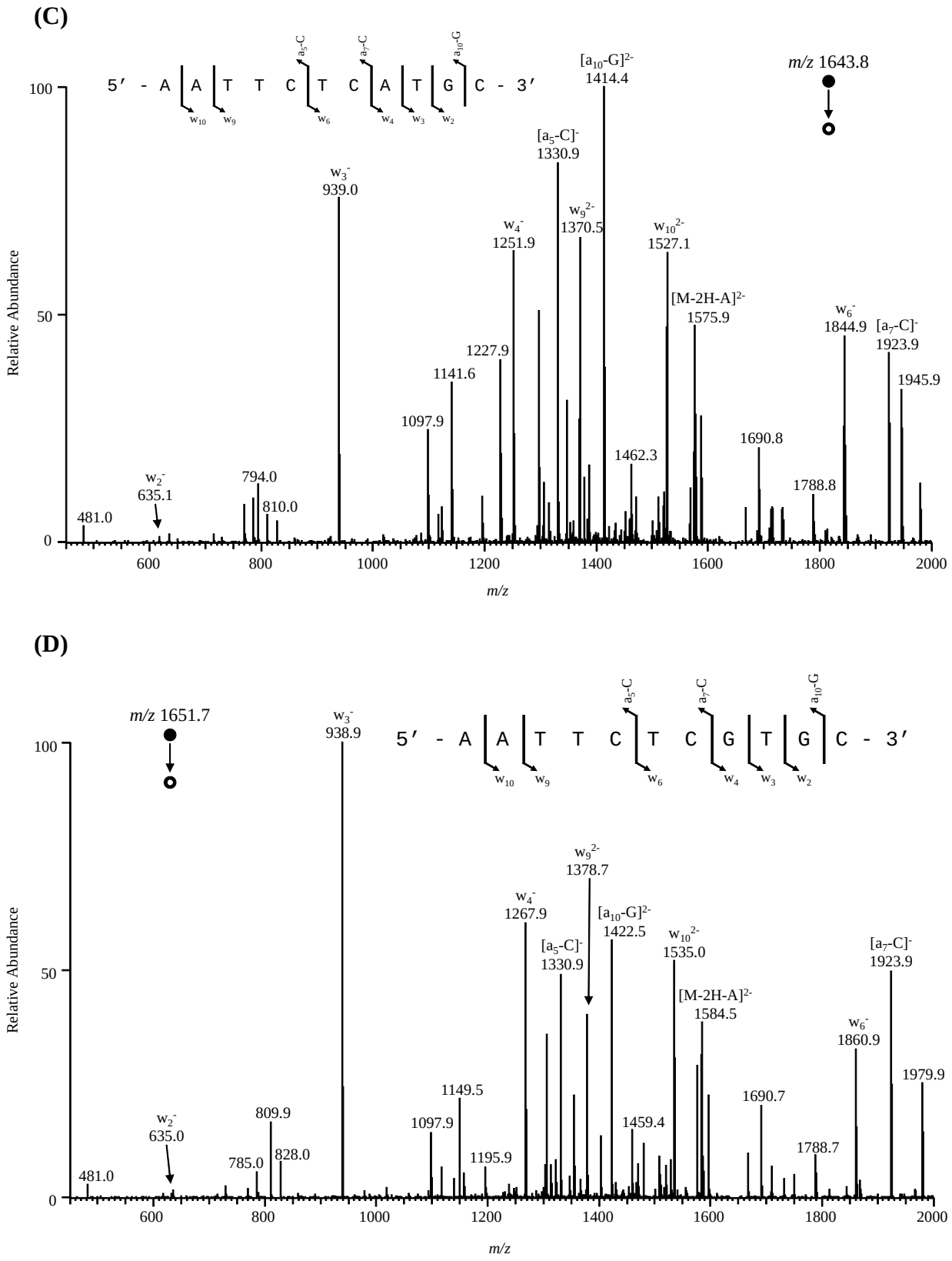
(C)
5′ - A A T T C T C A T G C - 3′
m/z 1643.8
[a10-G]2- 1414.4
[a5-C]- 1330.9
w3- 939.0
w9 2- 1370.5
w4- 1251.9
w10 2- 1527.1
[M-2H-A]2- 1575.9
w6- 1844.9
[a7-C]- 1923.9
1945.9
1227.9
1141.6
1097.9
1690.8
1462.3
1788.8
w2- 635.1
794.0
810.0
481.0
Relative Abundance
m/z
(D)
m/z 1651.7
w3- 938.9
5′ - A A T T C T C G T G C - 3′
w9 2- 1378.7
w4- 1267.9
[a10-G]2- 1422.5
[a5-C]- 1330.9
w10 2- 1535.0
[a7-C]- 1923.9
[M-2H-A]2- 1584.5
w6- 1860.9
1979.9
1149.5
1690.7
809.9
1097.9
1459.4
w2- 635.0
828.0
785.0
1195.9
1788.7
481.0
Relative Abundance
m/z

Figure S8.

(A)

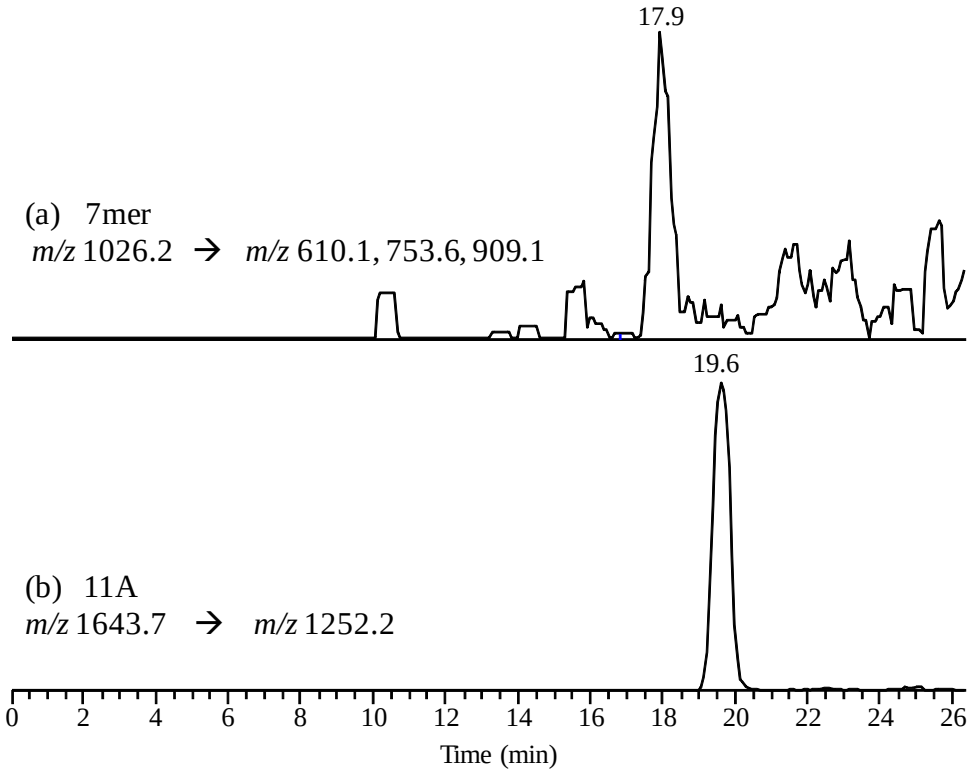


```
5′- GC AXG AGA ATT -3′
    3′-  C TCT TAA -5′     7mer      2%
3′- CG TAC TCT TAA -5′     11A       98%
```

dT Replication From Klenow fragment exo$^-$

Figure S9.

(B)

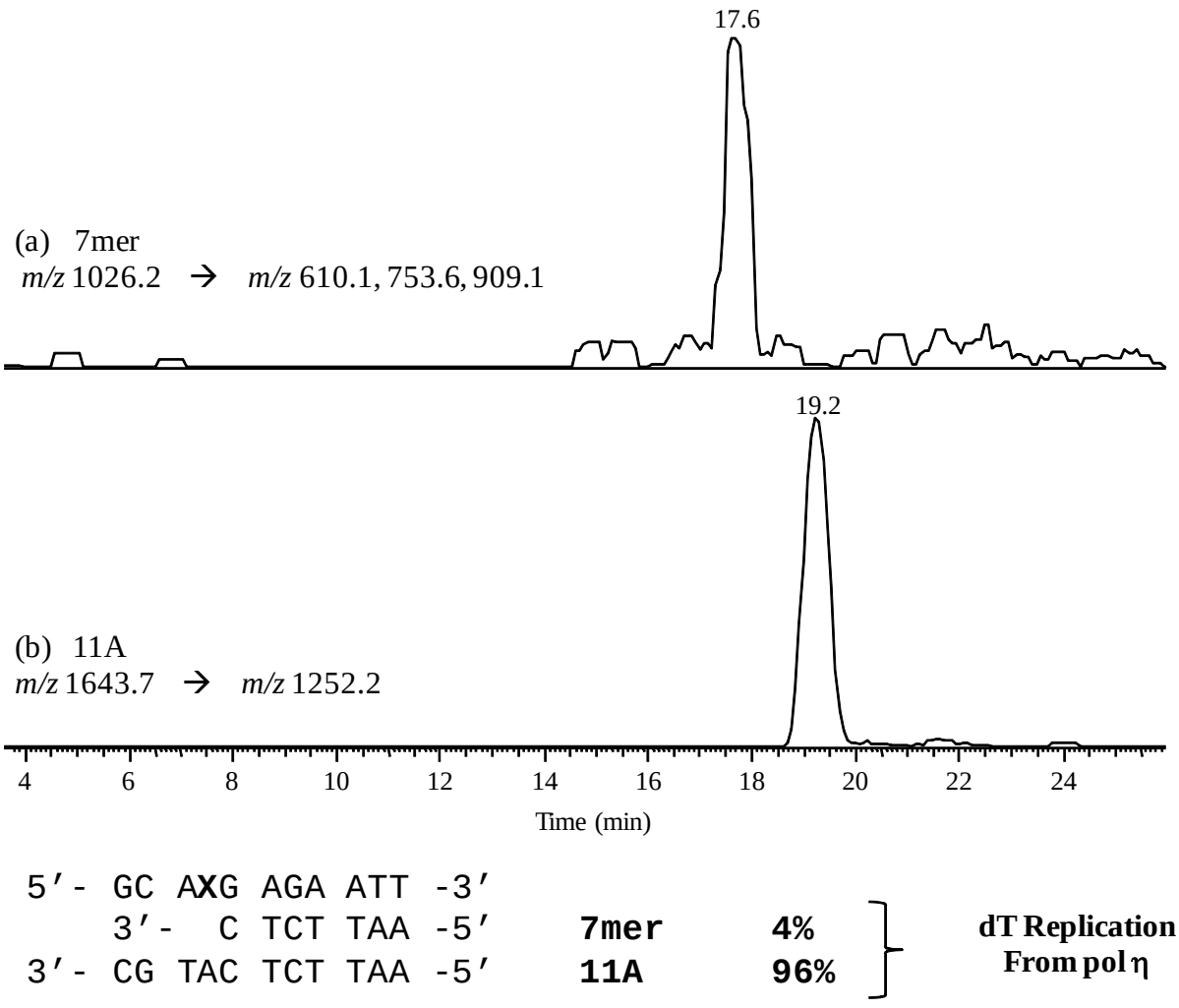
17.6
(a) 7mer
m/z 1026.2 → m/z 610.1, 753.6, 909.1
19.2
(b) 11A
m/z 1643.7 → m/z 1252.2
4
6
8
10
12
14
16
18
20
22
24
Time (min)
5′- GC AXG AGA ATT -3′
3′- C TCT TAA -5′ 7mer 4%
3′- CG TAC TCT TAA -5′ 11A 96%
dT Replication From pol η

Figure S9.

(C)

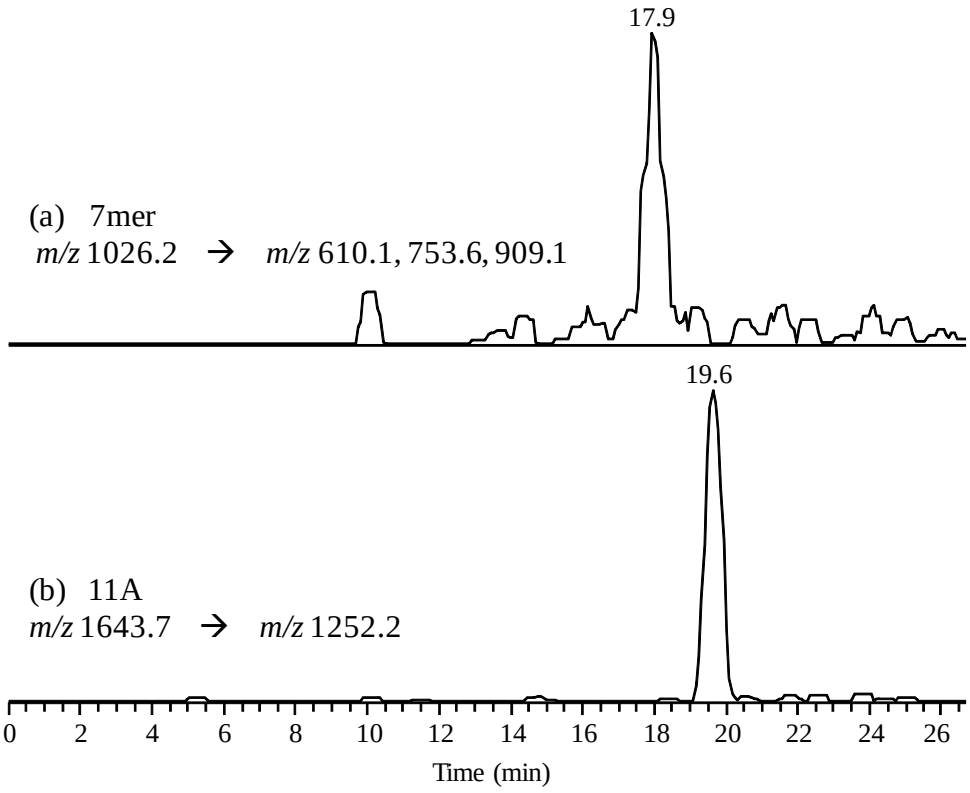

5′- GC AXG AGA ATT -3′
3′- C TCT TAA -5′ **7mer** **1%**
3′- CG TAC TCT TAA -5′ **11A** **99%**

dT Replication From polκ

Figure S9.

(A)

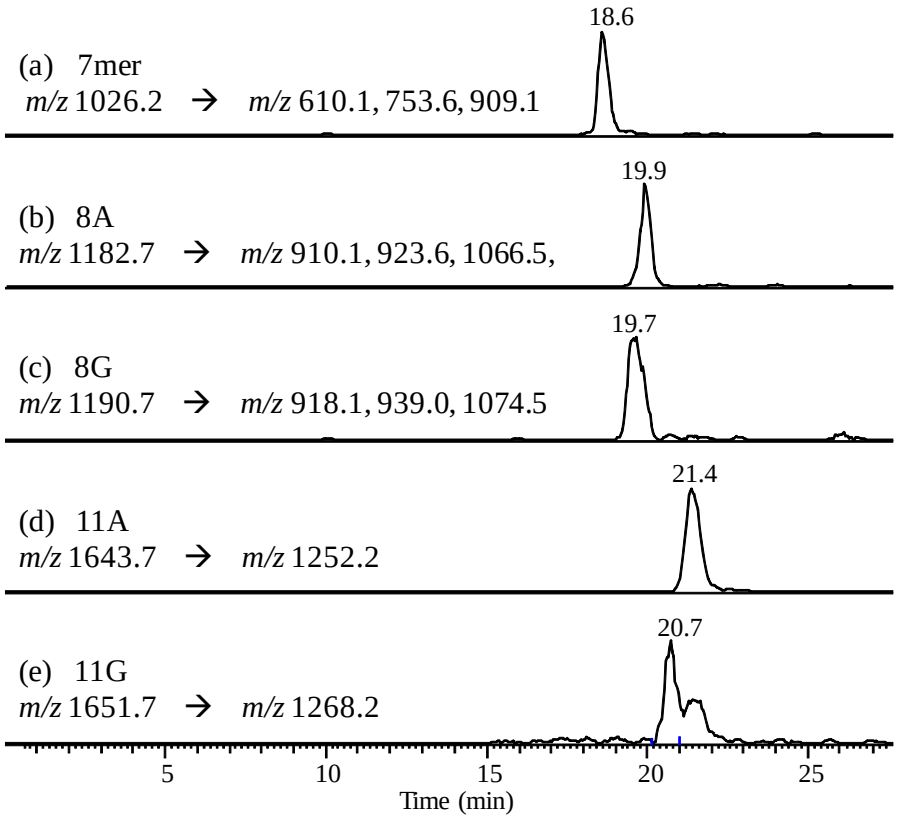

5′- GC AXG AGA ATT -3′		
3′- C TCT TAA -5′	**7mer**	**2%**
3′- AC TCT TAA -5′	**8A**	**9%**
3′- GC TCT TAA -5′	**8G**	**4%**
3′- CG TAC TCT TAA -5′	**11A**	**77%**
3′- CG TGC TCT TAA -5′	**11G**	**7%**

O^2-MdT Replication From Klenow fragment exo$^-$

Figure S10.

(B)

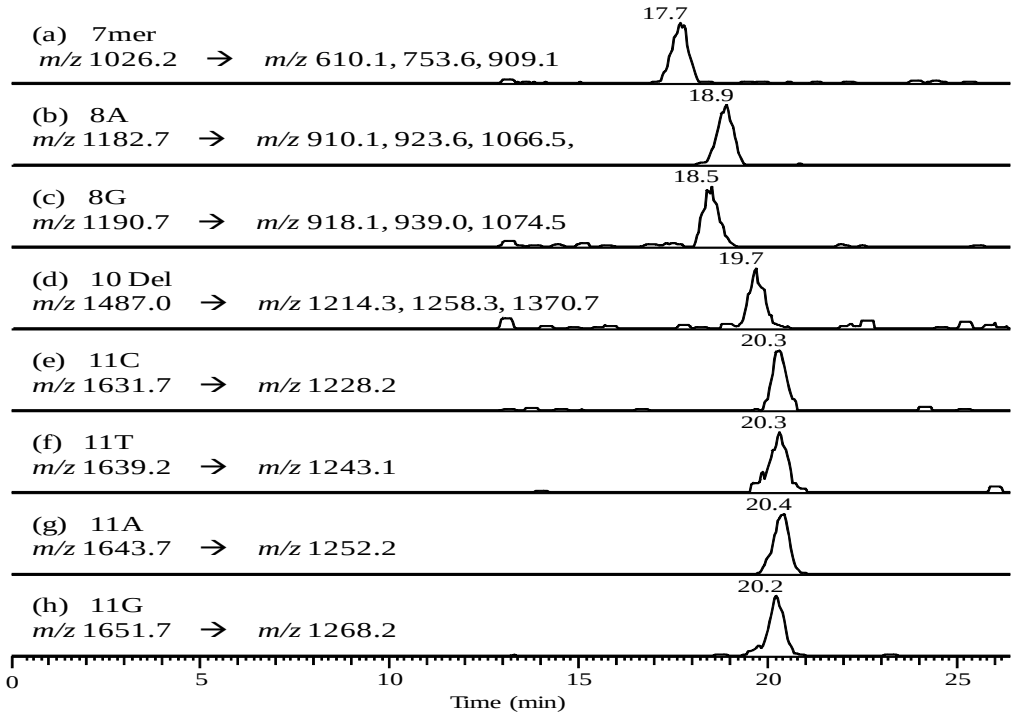

5′- GC AXG AGA ATT -3′		
3′- C TCT TAA -5′	**7mer**	**6%**
3′- AC TCT TAA -5′	**8A**	**2%**
3′- GC TCT TAA -5′	**8G**	**6%**
3′- CG T C TCT TAA -5′	**10Del**	**1%**
3′- CG TCC TCT TAA -5′	**11C**	**5%**
3′- CG TTC TCT TAA -5′	**11T**	**6%**
3′- CG TAC TCT TAA -5′	**11A**	**45%**
3′- CG TGC TCT TAA -5′	**11G**	**27%**

O^2-MdT Replication From pol η

Figure S10.

(A)

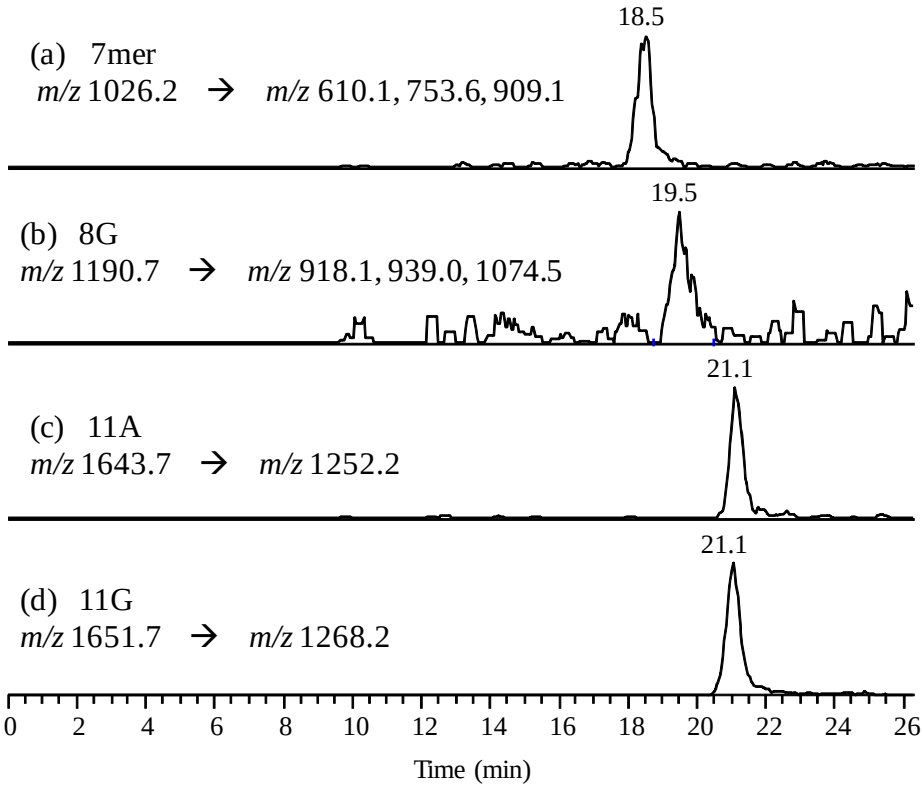

5′- GC AXG AGA ATT -3′		
3′- C TCT TAA -5′	**7mer**	**7%**
3′- GC TCT TAA -5′	**8G**	**5%**
3′- CG TAC TCT TAA -5′	**11A**	**7%**
3′- CG TGC TCT TAA -5′	**11G**	**80%**

O^4-MdT Replication From Klenow fragment exo$^-$

Figure S11.

(B)

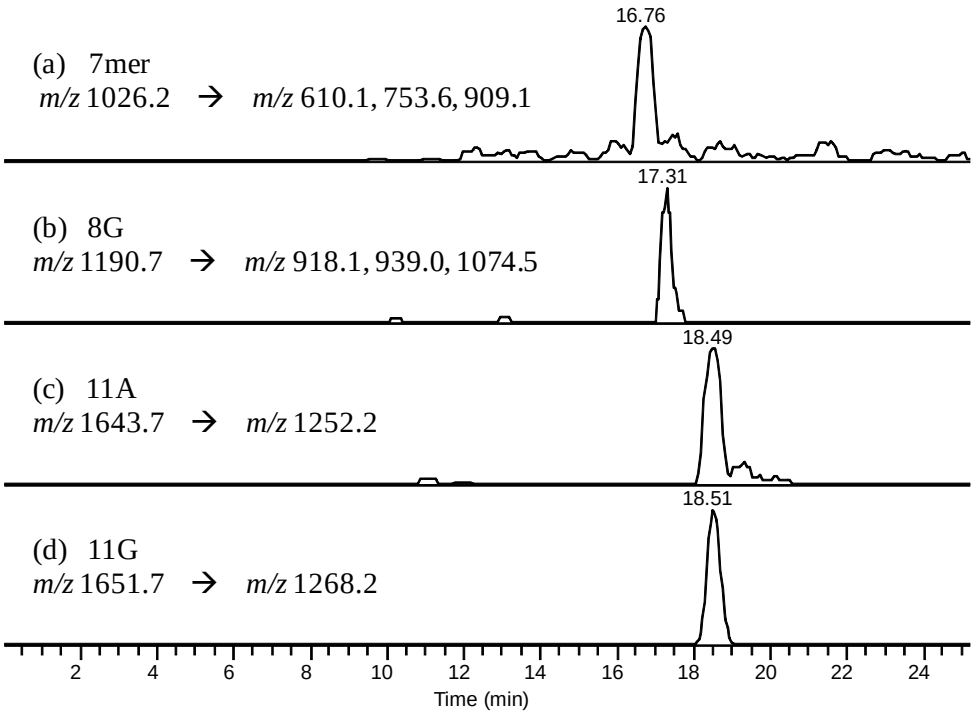

5′- GC AXG AGA ATT -3′		
3′- C TCT TAA -5′	**7mer**	**6%**
3′- GC TCT TAA -5′	**8G**	**2%**
3′- CG TAC TCT TAA -5′	**11A**	**9%**
3′- CG TGC TCT TAA -5′	**11G**	**83%**

O^4-MdT Replication From pol η

Figure S11.

(C)

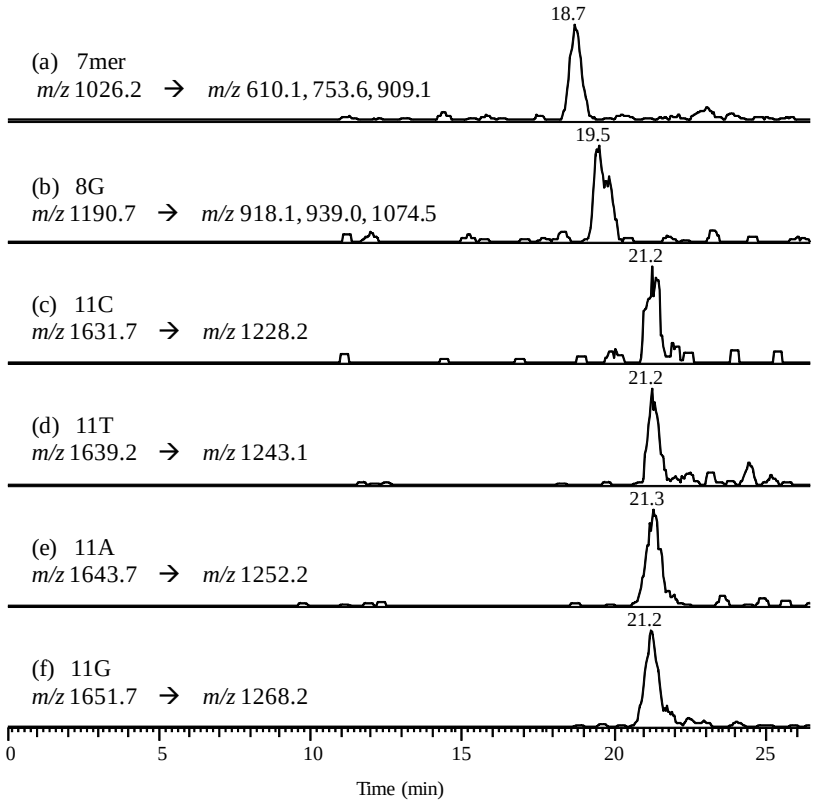

5′- GC A**X**G AGA ATT -3′		
3′- C TCT TAA -5′	**7mer**	**11%**
3′- GC TCT TAA -5′	**8G**	**18%**
3′- CG TCC TCT TAA -5′	**11C**	**2%**
3′- CG TTC TCT TAA -5′	**11T**	**3%**
3′- CG TAC TCT TAA -5′	**11A**	**8%**
3′- CG TGC TCT TAA -5′	**11G**	**58%**

O^4-MdT Replication From pol κ

Figure S11.

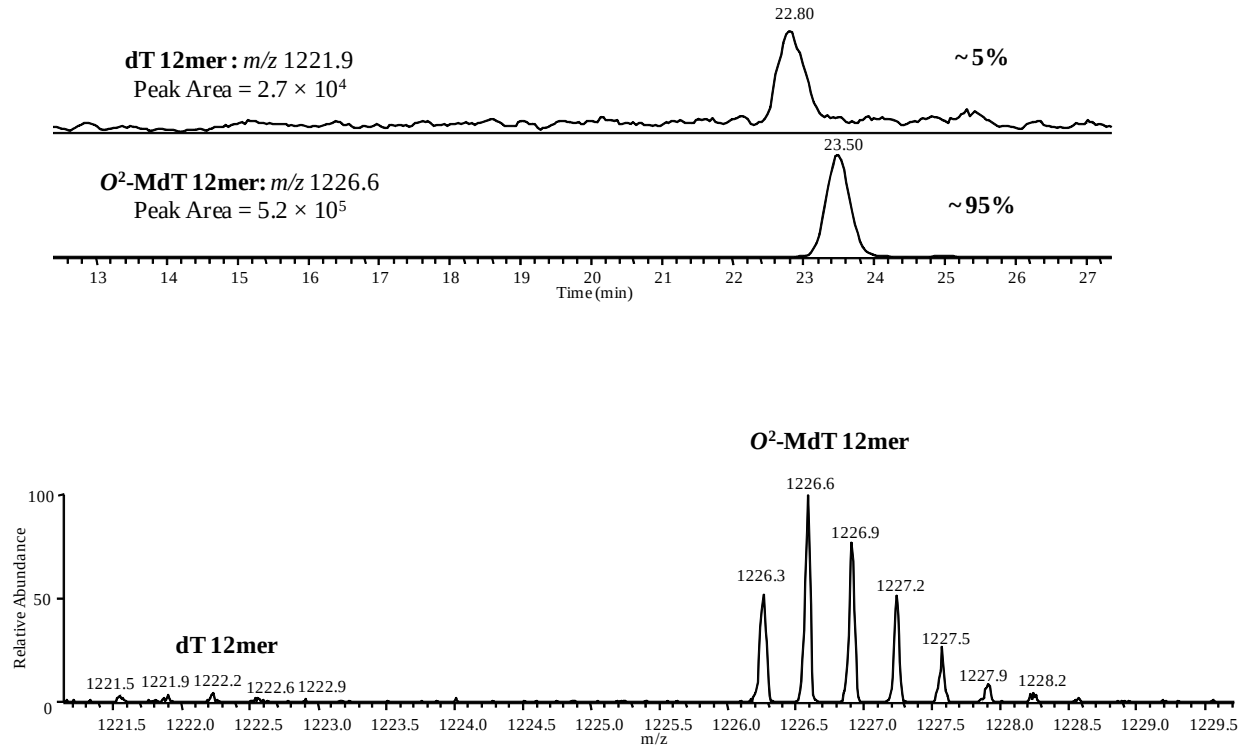
22.80
dT 12mer : m/z 1221.9
Peak Area = 2.7 × 10^4
~5%
23.50
O2-MdT 12mer: m/z 1226.6
Peak Area = 5.2 × 10^5
~95%
13 14 15 16 17 18 19 20 21 22 23 24 25 26 27
Time (min)
O2-MdT 12mer
1226.6
1226.9
1226.3
1227.2
1227.5
1227.9
1228.2
dT 12mer
1221.5 1221.9 1222.2 1222.6 1222.9
Relative Abundance
100
50
0
1221.5 1222.0 1222.5 1223.0 1223.5 1224.0 1224.5 1225.0 1225.5 1226.0 1226.5 1227.0 1227.5 1228.0 1228.5 1229.0 1229.5
m/z

Figure S12.

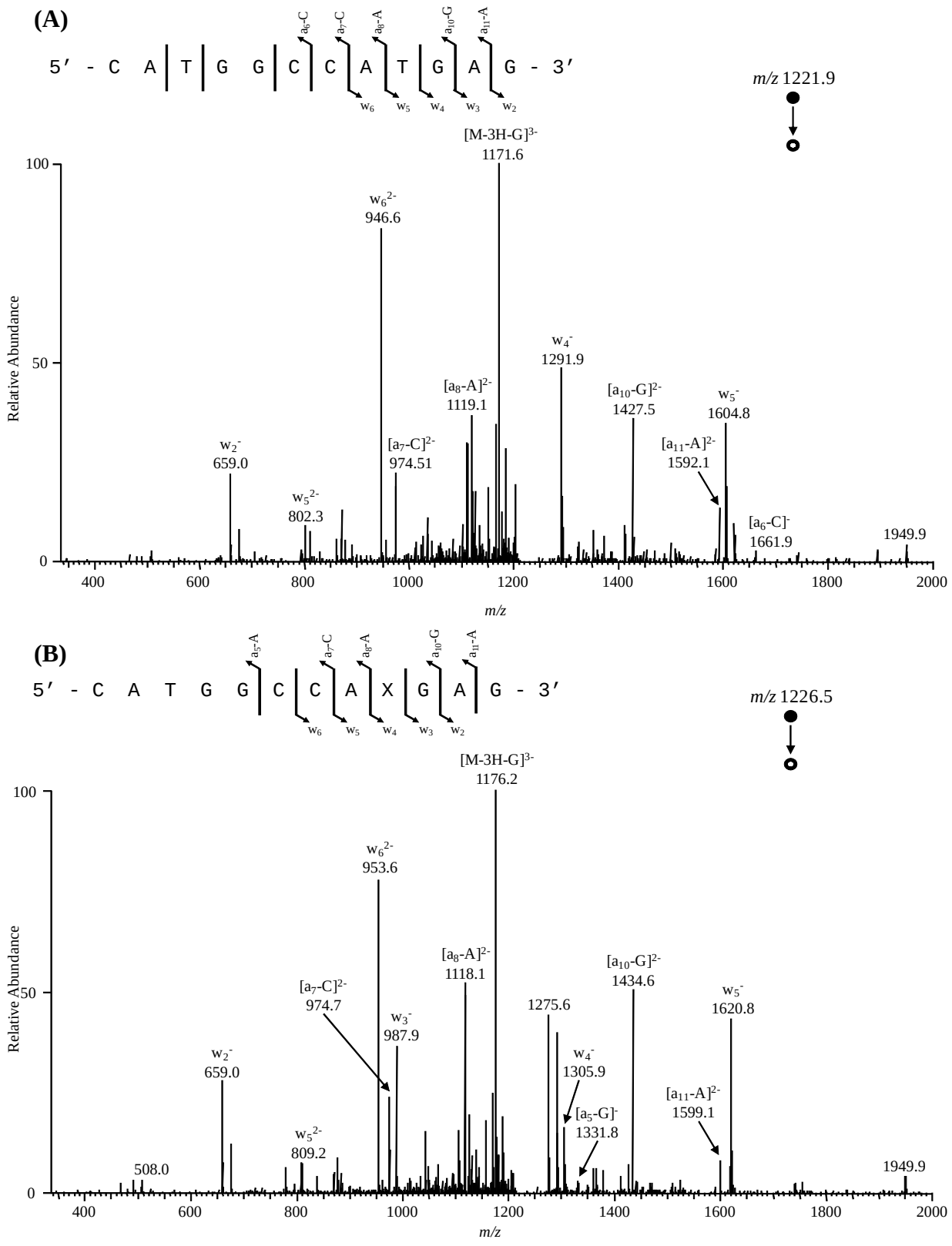
(A)
5′ - C A T G G C C A T G A G - 3′
a6-C
a7-C
a8-A
a10-G
a11-A
w6
w5
w4
w3
w2
m/z 1221.9
[M-3H-G]3-
1171.6
w6 2-
946.6
w4-
1291.9
[a8-A]2-
1119.1
[a10-G]2-
1427.5
w5-
1604.8
w2-
659.0
[a7-C]2-
974.51
[a11-A]2-
1592.1
w5 2-
802.3
[a6-C]-
1661.9
1949.9
Relative Abundance
m/z
(B)
5′ - C A T G G C C A X G A G - 3′
m/z 1226.5
[M-3H-G]3-
1176.2
w6 2-
953.6
[a8-A]2-
1118.1
[a10-G]2-
1434.6
[a7-C]2-
974.7
1275.6
w5-
1620.8
w3-
987.9
w4-
1305.9
w2-
659.0
[a5-G]-
1331.8
[a11-A]2-
1599.1
w5 2-
809.2
508.0
1949.9
Relative Abundance
m/z

Figure S13

(A)

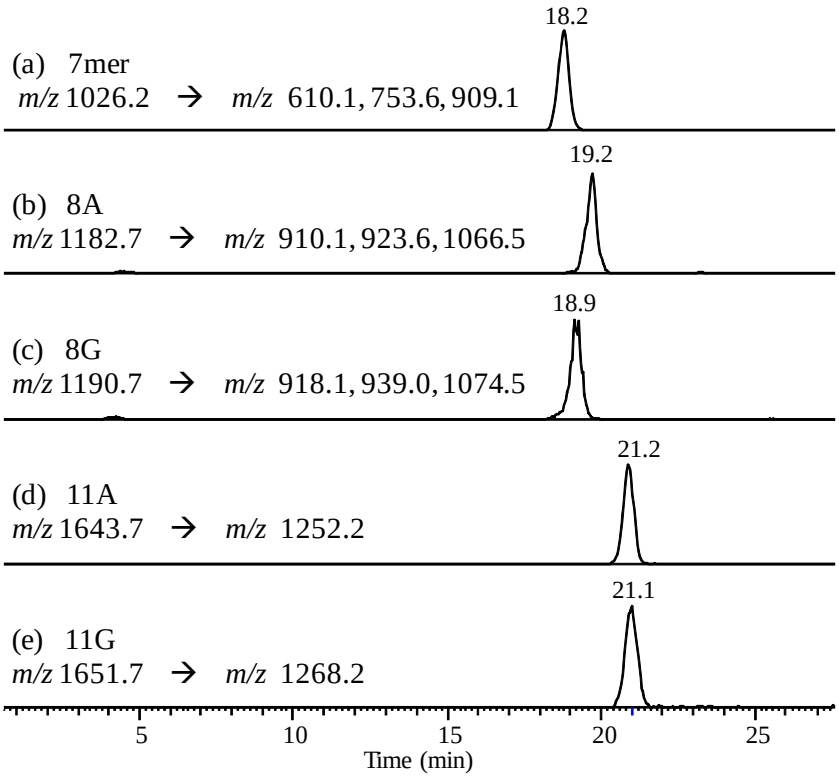

5′- GC A**X**G AGA ATT -3′		
3′- C TCT TAA -5′	**7mer**	**5%**
3′- AC TCT TAA -5′	**8A**	**3%**
3′- GC TCT TAA -5′	**8G**	**8%**
3′- CG TAC TCT TAA -5′	**11A**	**10%**
3′- CG TGC TCT TAA -5′	**11G**	**73%**

O^4-MdT Replication From pol η (low dNTPs)

Figure S14.

(B)

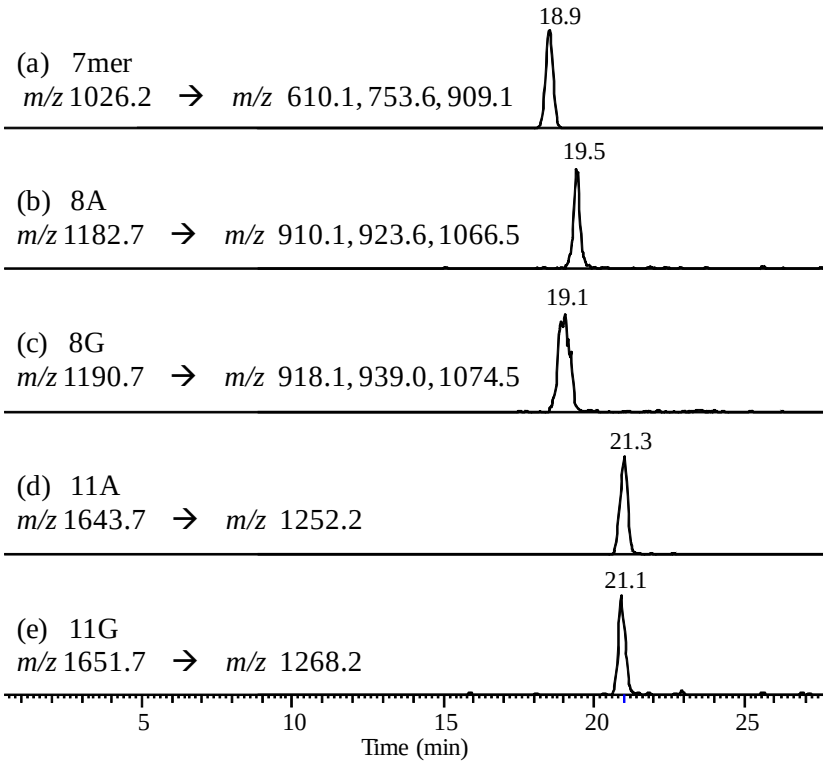

5′- GC AXG AGA ATT -3′		
3′- C TCT TAA -5′	**7mer**	**26%**
3′- AC TCT TAA -5′	**8A**	**3%**
3′- GC TCT TAA -5′	**8G**	**7%**
3′- CG TAC TCT TAA -5′	**11A**	**3%**
3′- CG TGC TCT TAA -5′	**11G**	**62%**

O^4-MdT Replication From pol η (6 hr)

Figure S14.

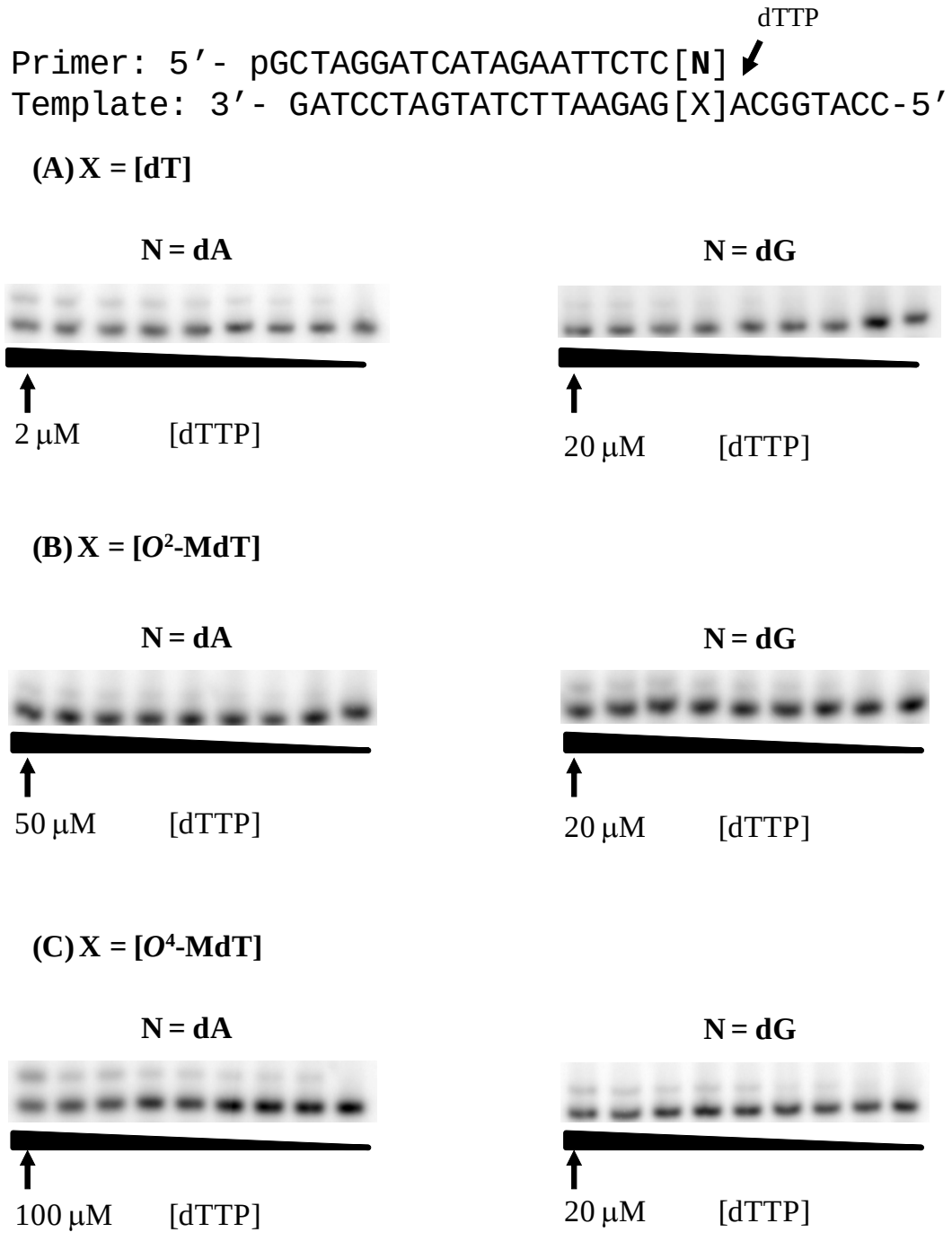
dTTP
Primer: 5′- pGCTAGGATCATAGAATTCTC[N]
Template: 3′- GATCCTAGTATCTTAAGAG[X]ACGGTACC-5′
(A) X = [dT]
N = dA
N = dG
2 μM [dTTP]
20 μM [dTTP]
(B) X = [O2-MdT]
N = dA
N = dG
50 μM [dTTP]
20 μM [dTTP]
(C) X = [O4-MdT]
N = dA
N = dG
100 μM [dTTP]
20 μM [dTTP]

Figure S15

Name	Sequence	O^4-MdT (low dNTPs)	O^4-MdT (6 hr)
	Yeast Polymerase η		
7mer	d(AATTCTC)	6	26
8mer	d(AATTCTCA)	3	3
8mer	d(AATTCTCG)	8	7
11A	d(AATTCTCATGC)	10	3
11G	d(AATTCTCGTGC)	73	62

Table S1.

dNTP	k_{cat} (min^{-1})	K_m (μM)	k_{cat}/K_m (mM^{-1} min^{-1})	f_{ext}
		Extension with dTTP		
dT:dATP	9.5 ± 0.4	0.56 ± 0.02	17	1
dT:dGTP	5.3 ± 0.1	2.2 ± 0.3	2.5	0.15
O^2-MdT:dATP	9.5 ± 0.4	7.8 ± 0.8	1.2	1
O^2-MdT:dGTP	13 ± 1	7.5 ± 0.5	1.7	1.4
O^4-MdT:dATP	10 ± 1	26 ± 2	0.38	1
O^4-MdT:dGTP	27 ± 2	11 ± 1	2	5.2

*The K_m and k_{cat} were average values based on three independent measurements

Table S2.